doi.org/10.36721/PJPS.2026.39.3.REG.14930.1

AKT inhibitor delays STZ-induced diabetic nephropathy by blocking EndoMT transformation

Yue Chen[1#], Yuanjing Li[2#] and Xing Wen[3]*

[1]Department of Oncology, Chongqing University Jiangjin Hospital, Chongqing, China
[2]Department of Nursing, Chongqing University Jiangjin Hospital, Chongqing, China
[3]Department of Nephrology and Rheumatology & Immunology, Chongqing University Jiangjin Hospital, Chongqing, China

Abstract: **Background**: Diabetic nephropathy (DN) is one of the most common and serious microvascular complications of diabetes, and a leading cause of end-stage renal disease. **Objective**: To investigate whether an AKT inhibitor can regulate EndoMT and participate in the pathogenesis of DN. **Methods**: Thirty Wistar rats were randomly divided into three groups: control, DN model, and AKT inhibitor VIII treatment (20 μM, administered daily via intravenous injection for 4 weeks). Levels of serum creatinine (Scr), blood urea nitrogen (BUN), urinary albumin (UAlb), reactive oxygen species (ROS), superoxide dismutase (SOD), inflammatory factors (IL-6, IL-1β), and the expression of EndoMT-related markers (VE-cadherin, CD31, α-SMA, collagen I) were measured. **Results**: Compared with the DN group, the AKT inhibitor significantly decreased the levels of Scr, BUN, UAlb, ROS, IL-6, IL-1β, TGF-β1, α-SMA, Collagen I and p-AKT ($P<0.05$), while it increased SOD activity and the expression of VE-Cadherin and CD31. **Conclusion**: The AKT inhibitor may delay the progression of diabetic nephropathy by inhibiting EndoMT, alleviating inflammation, and reducing oxidative stress.

Keywords: AKT; Diabetic nephropathy; EndoMT; Inhibitor; Inflammation; Oxidative stress

Submitted on 28-07-2025 – Revised on 21-11-2025 – Accepted on 01-12-2025

INTRODUCTION

Diabetic nephropathy (DN) is one of the most common and serious microvascular complications of diabetes and has become a leading cause of end-stage renal disease (Gupta *et al*., 2023; Samsu, 2021). Its characteristic pathological features include glomerulosclerosis, extracellular matrix accumulation and progressive renal fibrosis, ultimately leading to irreversible loss of renal function (Yoon *et al*., 2021; Tsuruta *et al*., 2024). Although current interventions such as blood glucose and blood pressure control can delay the progression of DN, they cannot effectively halt it. Therefore, it is crucial to elucidate the molecular mechanisms of DN and identify new therapeutic targets (Sugahara *et al*., 2021; Guo *et al*., 2024). The pathogenesis of DN is complex, with renal fibrosis being a central process. In recent years, the role of endothelial-to-mesenchymal transition (EndoMT) in renal fibrosis has garnered significant attention (Jacobs *et al*., 2024). EndoMT refers to the biological process in which vascular endothelial cells lose their specific markers (such as VE-Cadherin and CD31) under specific pathological stimuli and acquire a mesenchymal cell phenotype (such as expressing α-smooth muscle actin (α-SMA) and collagen I) (Yin and Wang, 2023). This transition disrupts the integrity of renal microvessels and directly contributes to the accumulation of fibroblasts, driving the fibrotic process.

Studies have shown that factors such as transforming growth factor-β1 (TGF-β1) can strongly induce EndoMT in diabetic kidneys (Song *et al*., 2022). Within the complex signaling network of the diabetic kidney, the AKT signaling pathway is regarded as a key regulatory hub. This pathway is not only involved in regulating cell metabolism, proliferation and survival but is also abnormally activated in the diabetic state (Yao *et al*., 2023; Zhang *et al*., 2021). Notably, AKT is a key downstream effector of TGF-β1 signaling and can interact with other critical pathogenic factors in DN, such as inflammation and oxidative stress (Feng *et al*., 2025; Xu *et al*., 2021). Theoretically, it is reasonable to hypothesize that excessive activation of AKT may mediate the initiation and progression of EndoMT in the diabetic environment. However, it remains unclear whether pharmacological inhibition of AKT can exert renal protective effects by directly intervening in the EndoMT process. This scientific question still awaits experimental confirmation.

Among the numerous AKT inhibitors, AKT inhibitor VIII (also known as a perifosine analog) was selected for our study due to its high selectivity and potent in vivo activity. It functions by inhibiting the phosphorylation of AKT and its kinase activity and has demonstrated anti-fibrotic potential in other kidney disease models (Ouyang *et al*., 2023; Feng *et al*., 2021). These properties make it an ideal pharmacological tool for investigating the role of AKT in DN.

Based on the aforementioned background, this study proposes the following hypothesis: In a streptozotocin (STZ)-induced diabetic nephropathy rat model, AKT inhibitor VIII can, by inhibiting AKT phosphorylation, subsequently block the EndoMT process, alleviate renal inflammation and oxidative stress and ultimately delay the progression of DN. To test this hypothesis, we systematically evaluated the effects of AKT inhibitor VIII

**Corresponding author:* e-mail: meihan9048980@126.com
[#]The authors contributed equally; therefore, they are the co-first authors

on renal function, inflammatory factors, oxidative stress markers and key EndoMT markers.

MATERIALS AND METHODS

Animals

Thirty Wistar rats, aged 12 weeks and weighing 250 ± 30 g, were from our animal center and maintained under a 12 h light/dark cycle with free access to food and water. AKT inhibitor VIII was from Shanghai Biyuntian Biotechnology Co., Ltd. The operating microscope was purchased from Jiangsu Zhenjiang Optical Instrument Company. Streptozotocin STZ was from Sigma, USA. ECL reagents were from Amersham Biosciences, mouse anti-rat Akt mAb and phosphorylated mAb were purchased from Cell Signaling, USA. IL-6 and IL-1β ELISA detection kits were purchased from American R&D Company.

Grouping

A solvent control group was not included, as preliminary experiments showed that the solvent did not significantly affect renal function indicators. To better highlight the drug effects, a three-group design was adopted. Thirty rats were randomly and equally divided into three groups (n=10 per group): the control group, the DN group and the AKT inhibitor VIII group. The DN model was induced by streptozotocin； The AKT inhibitor VIII group received AKT inhibitor VIII intravenously at a dose of 20 μM once daily for 4 weeks, based on prior pharmacodynamic and toxicity studies indicating that 20 μM is an effective and safe concentration in vivo, with intravenous administration ensuring bioavailability (He and Xu, 2022). The sample size was determined based on preliminary data and a power analysis using G*Power software (α=0.05, β=0.2, effect size f=0.4), which indicated that at least 8 animals per group were required. A final sample size of n=10 was set to enhance statistical robustness. Group allocation was performed using a random number table and blinded assessment was implemented during the experiments.

DN model preparation

One week after rats were adaptively reared, a model was prepared. Before preparation, rats were fasted for 12 hours and injected with 0.5% streptozotocin (40 mg/kg) via tail vein to prepare the model. Rats in the control group were injected with an equal volume of buffer solution. Model validation: Starting 72 hours after STZ injection, random blood glucose levels were monitored daily. At the 2nd and 4th weeks after STZ injection (i.e., before the initiation of AKT inhibitor treatment), we systematically assessed the stability of the model. A successful DN model was required to simultaneously meet the following three criteria: (1) random blood glucose concentration consistently higher than 16.7 mmol/L; (2) urine glucose test strip results persistently at "++" or above; and β significantly elevated 24-hour urinary albumin excretion (UAlb) compared to the control group (He and Xu, 2022).

Specimen collection

After treatment, the rat aorta blood was collected and placed for 30 minutes, followed by centrifugation to obtain the supernatant, which was placed at -20°C until use. Rats were euthanized, and the left kidney tissue was collected and stored at -80°C for further analysis.

Detection of renal function indicators of rats in each group

Serum creatinine (Scr) and blood urea nitrogen (BUN) levels were measured using a fully automated biochemical analyzer (Model: Polaris c2000; Manufacturer: Xi'an Tianlong Technology Co., Ltd.). Urinary albumin (UAlb) levels were determined by radioimmunoassay, with all procedures strictly following the instructions of the kit (UAlb Kit, Catalog Number: 2707100200; Manufacturer: Shanghai Enzyme-linked Biotechnology Co., Ltd.). Three technical replicates were set up for each sample to ensure data accuracy.

Analysis of changes in ROS content and SOD activity

Reactive oxygen species (ROS) content and superoxide dismutase (SOD) activity in renal tissues were measured using the ROS Assay Kit (Catalog Number: S0033S, Manufacturer: Beyotime Biotechnology, Shanghai) and the SOD Assay Kit (Catalog Number: S0101S, Manufacturer: Beyotime Biotechnology, Shanghai), respectively. Each experimental group included at least six biological replicates, with two technical replicates per sample.

ELISA

The concentrations of IL-6 and IL-1β in rat serum were measured strictly according to the instructions of the commercial ELISA kits. The details of the kits used are as follows: Rat IL-6 ELISA Kit (Catalog Number: KBI5030, Manufacturer: R&D Systems, USA); Rat IL-1β ELISA Kit (Catalog Number: AX53101, Manufacturer: R&D Systems, USA). All samples were tested in duplicate.

Real-time PCR

Total RNA was extracted from renal tissues using the TRIzol method. One microgram of RNA was reverse-transcribed into cDNA using a reverse transcription kit (PrimeScript RT Reagent Kit, Catalog Number: RR047A, Manufacturer: TaKaRa). Subsequently, amplification was performed on a real-time quantitative PCR instrument (Model: ABI 7500) using SYBR Green Premix (TB Green Premix Ex Taq II, Catalog Number: RR820A, Manufacturer: TaKaRa). The reaction protocol was as follows: 95°C for 30 seconds; followed by 40 cycles of 95°C for 5 seconds and 60°C for 34 seconds. GAPDH was used as the internal reference gene and the relative mRNA expression levels of the target genes were calculated using the $2^{-\Delta\Delta Ct}$ method. Three technical replicates were set up for each sample. The primer sequences for RT-PCR are listed in table 1.

Table 1: Primer sequences.

Gene	Forward 5'-3'	Reverse 5'-3'	Source/Design method
GAPDH	ACCAGGTATCTTGGTTGTC	TAACCATGTCAGCGTGGTCA	Reference (Park *et al*., 2024)
TGF-β1	CAGTAGTGGTCTCTACCGCC	TCATTAACCCTCTCACAGAACC	Self-designed and validated by Primer-BLAST.
VE-Cadherin	CTCATCACAGTAATGGCTGT	GCACCTTAGGTTCCGATCTG	Reference (Lee *et al*., 2022)
CD31	TAAGAGGAGGACAATGGCTG	ACATCATTCATCTTCTGCCG	Reference (Guan *et al*., 2025)
α-SMA	TAAAGGAAGCGGAATGGCTG	ACATCATCTATTCTCTTGTCGG	Reference (Karetnikova *et al*., 2023)
Collagen I	CAACTACCGCTCGCTTAAG	GCACTGGATTGACCTTTGTGA	Self-designed and validated by Primer-BLAST.

Table 2: General indicators and renal function tests of rats in each group.

Parameters	Control	DN	AKT inhibitor
Weight (g)	453.4±48.8	242.5±32.5*	331.6±37.5*#
Blood sugar (mmol/L)	6.8±0.9	26.5±5.5*	16.2±2.5*#
Kidney/weight (mg/g)	2.3±0.6	4.7±0.6*	3.1±0.4*#
Scr (μmol/L)	121.8±12.5	1051.2±72.6*	721±59.6*#
BUN (mmol/L)	5.9±0.8	15.1±1.8*	9.9±1.8*#
UAlb (mg/24h)	0.6±0.2	1.9±0.5*	1.0±0.4*#

Note: Compared with the control group, * $P < 0.05$; compared with the DN group, #$P < 0.05$.

Western blot

Total protein was extracted from renal tissues and quantified using the BCA method. Equal amounts of protein (30 μg) were separated by SDS-PAGE and subsequently transferred to PVDF membranes. After blocking with 5% skimmed milk, the membranes were incubated overnight at 4℃ with specific primary antibodies. The primary antibodies used included: p-AKT (Ser473) antibody (rabbit monoclonal, Catalog No.: TDCCR-1081, Manufacturer: Wuhan Tiande Co., Ltd., dilution 1:1000); total AKT antibody (rabbit monoclonal, Catalog No.: IPD-ANP1053, Manufacturer: Aptibiotech, dilution 1:1000); and GAPDH antibody (mouse monoclonal, Catalog No.: 80151-MM01-F, Manufacturer: Beijing Sino Biological Inc., dilution 1:5000). The following day, the membranes were incubated with corresponding HRP-conjugated secondary antibodies at room temperature for 1 hour. Finally, protein bands were visualized using an ECL chemiluminescence reagent (Amersham ECL Prime, Catalog No.: GK10008, Manufacturer: GlpBio, USA). Each experimental condition was repeated in at least three independent experiments (n=3).

Statistical analysis

Data analysis was performed using SPSS 19.0 software. All data were confirmed to follow a normal distribution by the Shapiro-Wilk test and homogeneity of variances by Levene's test. Data are expressed as mean ± standard deviation (SD). Intergroup comparisons were conducted using one-way analysis of variance (ANOVA), with post-hoc testing performed using Tukey's method. A P-value < 0.05 was considered statistically significant.

RESULTS

AKT inhibitors' effect on the survival status and renal function of DN rats

The body weight of DN rats was reduced, while the kidney-to-body weight ratio, Scr, BUN, and UAlb were significantly increased ($P < 0.05$) and treatment with AKT inhibitor could significantly improve the general state and hair color and increase the weight and reduce Scr, BUN, UAlb ($P < 0.05$) (Table 2).

Effect of AKT inhibitor on inflammatory secretion factors in serum of DN rats

In DN group, IL-6 and IL-1β were increased ($P < 0.05$) and decreased after AKT inhibitor treatment ($P < 0.05$) (Fig. 1).

Effect of AKT inhibitor on the expression of TGF-β1

Real-time PCR showed that TGF-β1 levels were significantly elevated in the renal tissue of DN group rats ($P < 0.05$). AKT inhibitor significantly inhibited TGF-β1 expression ($P < 0.05$) (Fig. 2).

Effect of AKT inhibitor on oxidative stress

The changes of ROS content and SOD activity in renal tissues after DN rats and AKT inhibitor treatment were analyzed. The results confirmed that the ROS content in DN group was increased and SOD activity was decreased ($P < 0.05$), which were reversed by AKT inhibitor ($P < 0.05$) (Fig. 3).

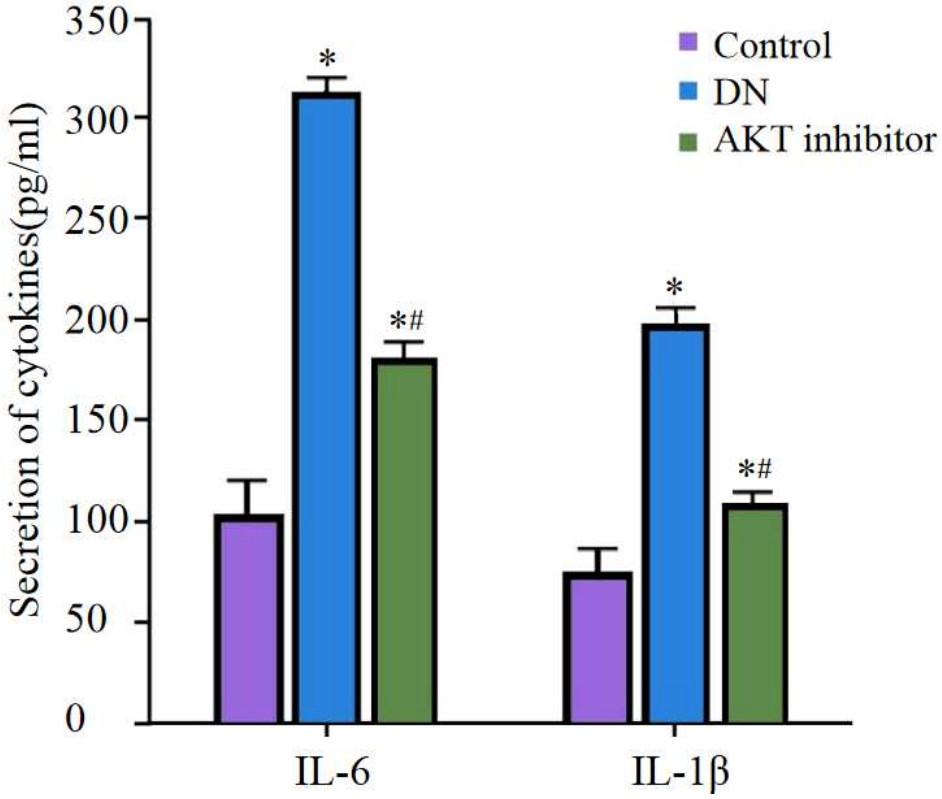

Fig. 1: AKT inhibitor VIII ameliorates systemic inflammation in DN rats. Serum levels of inflammatory cytokines IL-6 and IL-1β were measured by ELISA. Induction of the DN model significantly elevated pro-inflammatory cytokine levels, while treatment with AKT inhibitor VIII effectively reversed this trend. Data are presented as mean ± standard deviation (n=10). *P < 0.05 compared with the control group; #P < 0.05 compared with the DN group.

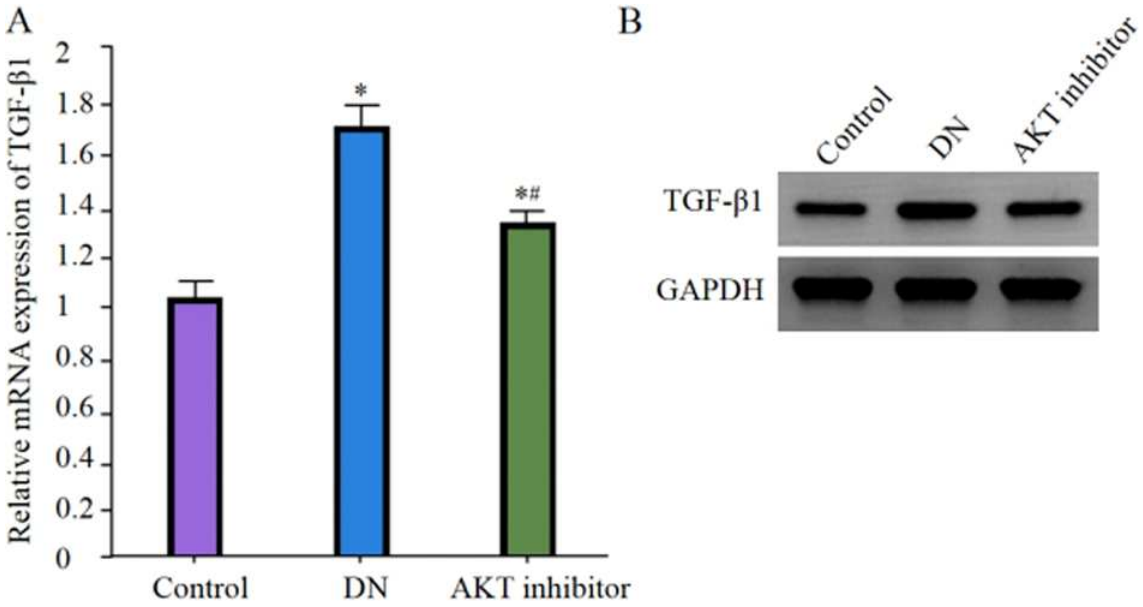

Fig. 2: Effects of AKT inhibitor on renal TGF-β1 expression in diabetic nephropathy rats. **(**A) TGF-β1 mRNA expression levels; (B) Representative Western blot images of TGF-β1 protein. TGF-β1 expression was significantly upregulated in the DN group, while AKT inhibitor treatment markedly suppressed this renal fibrotic progression. Data are presented as mean ± SD (n=10). *P < 0.05 vs. control group; #P < 0.05 vs. DN group.

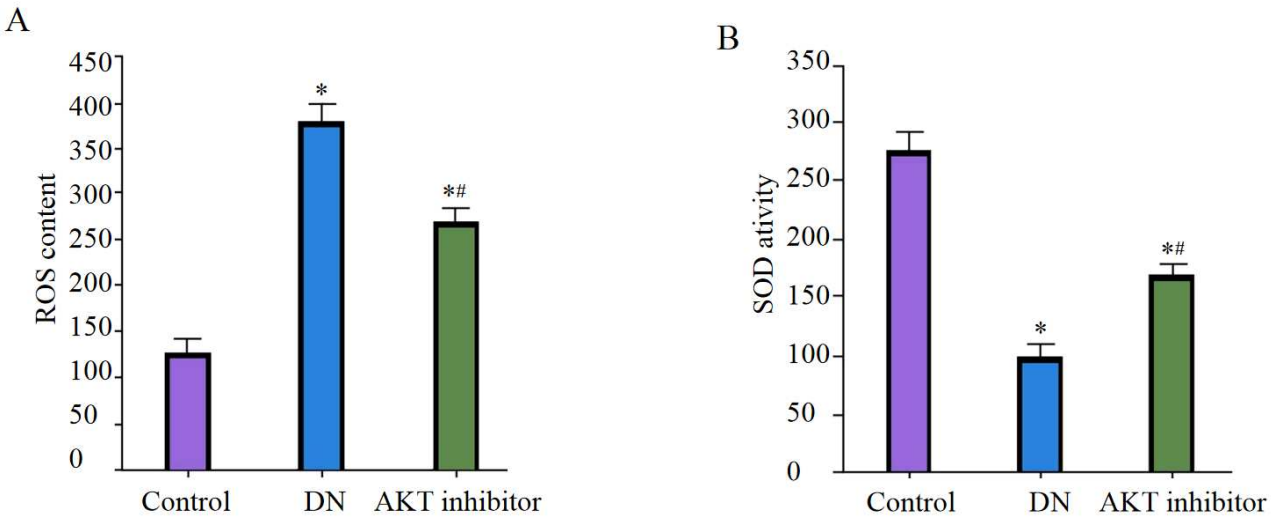

Fig. 3: Effect of AKT inhibitor on oxidative stress in kidney tissue of DN rats. (A) ROS content; (B) SOD activity. The DN group exhibited a significant increase in ROS content, while AKT inhibitor intervention markedly reduced ROS levels, suggesting that the inhibitor may exert renal protective effects by alleviating oxidative stress. SOD activity was significantly decreased in the DN group, indicating impaired antioxidant defense systems. Following AKT inhibitor intervention, SOD activity showed a significant recovery compared to the DN group, suggesting that the inhibitor mitigates oxidative stress damage by enhancing the body's intrinsic antioxidant capacity. Data are presented as mean ± standard deviation (n=10). compared with control group, * $P < 0.05$; compared with DN group, #$P < 0.05$.

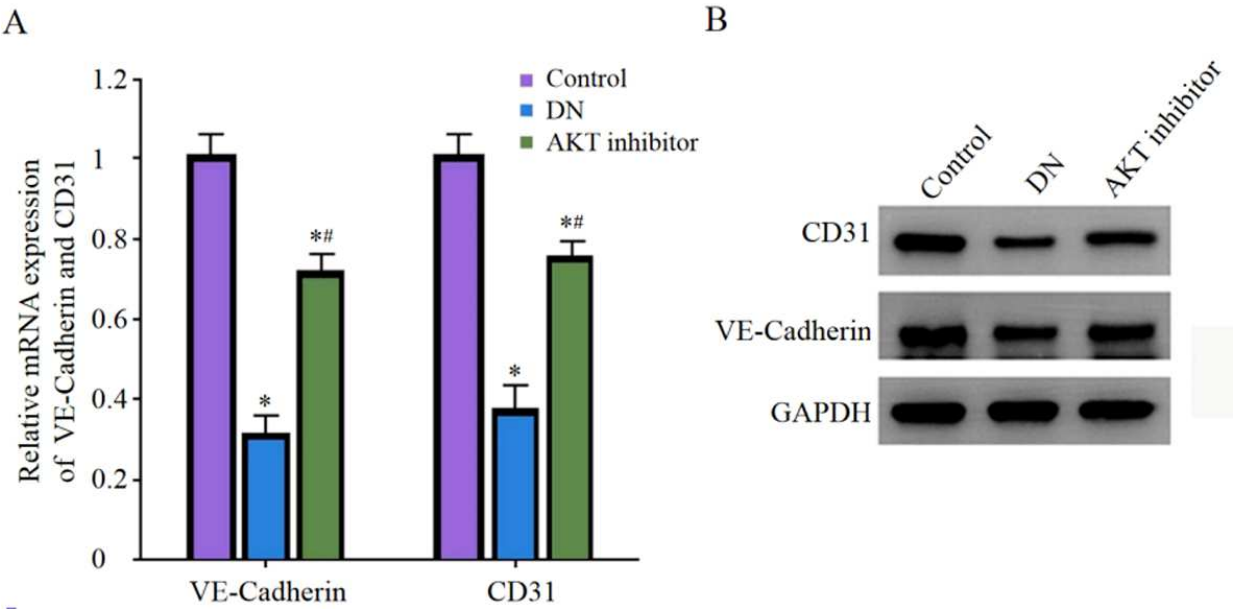

Fig. 4: Effect of AKT inhibitors on expression of vascular endothelial cell markers in kidney tissue of DN rats. (A) mRNA expression levels of VE-Cadherin and CD31; (B) Western blot images of VE-Cadherin and CD31 proteins. In the DN group, the mRNA expression levels of both VE-Cadherin and CD31 were significantly downregulated. However, after intervention with the AKT inhibitor, the expression levels of these two markers significantly recovered compared to the DN group. This suggests that the AKT inhibitor may exert renal protective effects in diabetic nephropathy by preserving vascular endothelial cells and promoting endothelial repair. Data are presented as mean ± standard deviation (n=10). Compared with the control group, * $P < 0.05$; compared with the DN group, #$P < 0.05$.

Effect of AKT inhibitor on the expression of vascular endothelial cell markers

Expression of VE-Cadherin and CD31 in DN rats was significantly downregulated ($P < 0.05$) and AKT inhibitor can significantly upregulate VE-Cadherin and CD31 ($P < 0.05$) (Fig. 4).

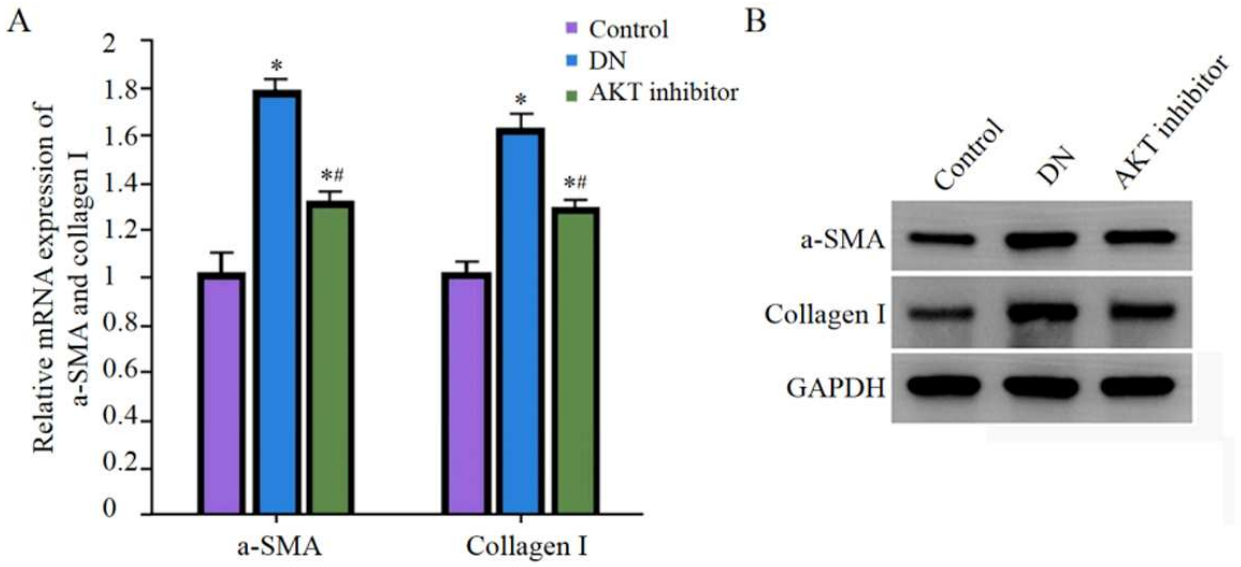

Fig. 5: Effect of AKT inhibitors on expression of mesenchymal cell markers in kidney tissue of DN rats. (A) mRNA expression levels of α-SMA and Collagen I; (B) Western blot images of α-SMA and Collagen I proteins. In the DN group, the mRNA expression levels of both α-SMA and Collagen I were significantly upregulated. After intervention with the AKT inhibitor, the expression levels of these two markers were significantly reduced compared to the DN group. This suggests that the AKT inhibitor may delay or alleviate renal fibrosis in diabetic nephropathy by inhibiting the activation of myofibroblasts and the excessive accumulation of extracellular matrix. Data are presented as mean ± standard deviation (n=10). Compared with the control group, * P < 0.05; compared with the DN group, #P < 0.05.

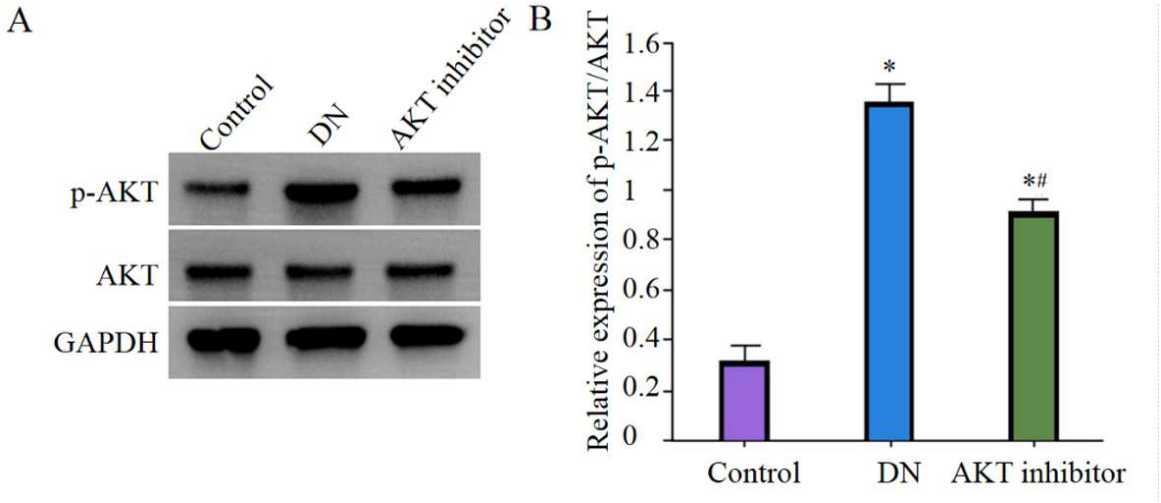

Fig. 6: Effect of AKT inhibitor on AKT expression in kidney tissue of DN rats. (A) Protein immunoblots results; (B) Relative expression of p-AKT/AKT. The p-AKT/AKT ratio was significantly increased in the DN group, indicating abnormal activation of the AKT signaling pathway in diabetic nephropathy, which may promote renal cell hypertrophy, inflammation, and fibrosis. In the AKT inhibitor intervention group, this ratio was significantly reduced compared to the DN group, confirming that the inhibitor effectively suppressed the hyperactivation of the AKT pathway. Data are presented as mean ± standard deviation (n=10). compared with the control group, * P <0.05; compared with the DN group, #P < 0.05.

Effect of AKT inhibitor on expression of mesenchymal cell markers

α-SMA and Collagen I in DN rats were increased (P <0.05) and AKT inhibitor significantly inhibited α-SMA and Collagen I level (P <0.05) (Fig. 5).

Effects of AKT inhibitor on AKT signaling pathway activity

To validate the *in-vivo* efficacy of AKT inhibitor VIII, we analyzed the levels of total AKT and its phosphorylated form (p-AKT, Ser473) in renal tissues by Western blot. As

shown in fig. 6A, compared with the control group, the p-AKT protein levels were significantly increased in the kidneys of DN model rats, while the total AKT protein levels remained unchanged. Treatment with AKT inhibitor VIII significantly suppressed the p-AKT levels, whereas total AKT levels remained unaltered. Fig. 6B presents the quantitative analysis results from three independent experiments (all data were normalized to GAPDH), confirming the above observations ($P < 0.05$).

DISCUSSION

Diabetic nephropathy leads to renal hemodynamic disorders and glomerular basement membrane thickening, kidney hypertrophy. The increase of extracellular matrix causes dysfunction of endothelial cells, which in turn causes irreversible renal failure (Kushwaha *et al*., 2022). Therefore, finding a target is beneficial to the treatment of DN and can effectively improve patients' life quality. This study demonstrates that in an STZ-induced diabetic nephropathy rat model, AKT inhibitor VIII significantly improves renal function, alleviates oxidative stress and inflammatory responses and reverses the expression of EndoMT-related markers. More importantly, we found that these protective effects are closely associated with the inhibition of the AKT signaling pathway, providing new insights into understanding the pathogenesis of DN and developing potential therapeutic strategies.

The data from this study demonstrate that the DN group exhibited a significant increase in AKT phosphorylation levels, accompanied by characteristic changes of EndoMT such as downregulation of endothelial markers and upregulation of mesenchymal markers. AKT inhibitor VIII, while suppressing p-AKT, reversed these phenotypic changes. This strongly suggests that activation of the AKT pathway is a critical driver of the EndoMT process in DN. We hypothesize that the underlying mechanism is as follows: pathological factors such as hyperglycemia and TGF-β1 activate AKT, which may then initiate the EndoMT program by regulating downstream effectors such as glycogen synthase kinase-3β (GSK-3β) and transcription factors Snail/Slug (Li *et al*., 2021; Hu *et al*., 2025). AKT-mediated phosphorylation of GSK-3β inhibits its activity, thereby stabilizing Snail and other proteins and promoting the loss of endothelial markers such as VE-cadherin—a core step in EndoMT (Huang *et al*., 2022; Cui *et al*., 2021).

Furthermore, the results of this study confirm that the AKT inhibitor significantly suppresses the expression of TGF-β1. As a key inducer of EndoMT, TGF-β1 signaling regulates the expression of transcription factors Snail and Twist through the Akt/GSK-3β axis, thereby promoting the transition of endothelial cells to a mesenchymal phenotype (Xu *et al*., 2024). Thus, the AKT inhibitor may disrupt the phosphorylation state of GSK-3β, inhibit the nuclear translocation of Snail/Twist and consequently block the EndoMT process (Su *et al*., 2023). This suggests that the AKT inhibitor potentially restores GSK-3β activity, facilitates the degradation of Snail and ultimately helps maintain endothelial phenotypic stability.

Concurrently, the AKT inhibitor in this study significantly reduced the levels of IL-6 and IL-1β. The underlying mechanism for this observation may involve the ability of Akt to promote the nuclear translocation of NF-κB by activating the IKK complex, thereby inducing the expression of inflammatory cytokines (Cai *et al*., 2022). Furthermore, IL-6 itself can promote EndoMT via the JAK/STAT signaling pathway (Jing *et al*., 2025). Although the JAK/STAT pathway was not directly examined in this study, the inhibition of Akt, as an upstream regulator, likely attenuates both NF-κB and JAK/STAT signaling. This dual inhibition potentially creates a synergistic effect in suppressing both inflammation and the EndoMT process.

Additionally, the results of this study demonstrate that the AKT inhibitor reduces ROS levels and enhances SOD activity, which may be partially attributed to its modulation of the Akt/FOXO signaling axis. Under diabetic conditions, hyperactivated AKT phosphorylates FOXO transcription factors, leading to their cytoplasmic retention and degradation, thereby impairing FOXO-mediated transcriptional expression of antioxidant stress genes such as SOD. Inhibiting AKT may restore FOXO transcriptional activity, thereby strengthening cellular antioxidant defense mechanisms. Simultaneously, ROS itself can act as a second messenger to amplify TGF-β1 signaling, forming a positive feedback loop that further promotes EndoMT. Thus, the AKT inhibitor may disrupt this vicious cycle by modulating the Akt/FOXO axis, alleviating oxidative stress-driven renal fibrosis.

By employing AKT inhibitor VIII, this study confirms a significant association between the inhibition of AKT phosphorylation and the reversal of EndoMT, as well as the mitigation of inflammation and oxidative stress. However, it should be noted that although AKT inhibition and EndoMT reversal were temporally correlated, this study lacks cell-specific Akt knockout or pathway rescue experiments, preventing a definitive conclusion that AKT is the direct and specific driver of EndoMT reversal. Furthermore, as with any small-molecule inhibitor, potential off-target effects cannot be ruled out and the observed beneficial effects of AKT inhibitor VIII may not be solely attributable to AKT inhibition. Future studies should incorporate cell-specific genetic manipulation techniques to more precisely elucidate the role of Akt in EndoMT.

The complexity of pharmacological effects must also be thoroughly considered. This study observed that AKT inhibition concurrently improved hyperglycemia, suggesting that the observed renal protective effects may partially stem from systemic metabolic improvements

rather than solely from direct inhibition of renal AKT. To definitively demonstrate that AKT signaling directly drives EndoMT in renal cells, future research must employ cell-specific Akt knockout animal models or *in-vitro* co-culture systems to validate these findings under rigorously controlled conditions.

It is noteworthy that the AKT inhibitor not only reduced Scr and BUN levels but also downregulated the expression of pro-fibrotic genes, Collagen I and α-SMA. This suggests that its beneficial effect on renal function is likely mediated through the suppression of renal fibrosis, including the specific mechanism of EndoMT. However, this study does not provide renal histopathological sections that visually demonstrate the expansion of glomerular mesangial matrix, tubular atrophy, or the degree of interstitial fibrosis, which would have allowed a more direct correlation between the observed biochemical changes and specific morphological evidence of tissue damage. Although renal injury was assessed indirectly via functional markers and fibrogenic gene expression, future studies incorporating histological analysis would strengthen the conclusions.

CONCLUSION

EndoMT transformation and AKT activation occur during the development of diabetic nephropathy. AKT inhibitor blocks EndoMT transformation, inhibits inflammation, regulates oxidative stress and delays the progression of diabetic nephropathy. Future studies should employ gene knockout technology to precisely elucidate the role of AKT in specific cell types, such as renal endothelial cells. Additionally, exploring the combination of AKT inhibitors with existing standard therapies and developing more kidney-targeted formulations will be crucial for translating these novel therapeutic strategies into clinical practice.

Acknowledgment
We gratefully acknowledge Chongqing University Jiangjin Hospital for providing the necessary equipment for this study.

Author's contributions
Yue Chen: Conceptualization, methodology, data curation, formal analysis, writing - original draft; Yuanjing Li: Investigation, validation, data curation; Xing Wen: Supervision, writing - review & editing.

Funding
None

Data availability statement
The datasets generated and/or analyzed during the current study are available from the corresponding author on reasonable request.

Ethical approval
This study was approved by the ethics committee of Chongqing University Jiangjin Hospital (No. CQ20240502).

Conflict of interest
The authors declare that the research was conducted in the absence of any commercial or financial relationships that could be construed as a potential conflict of interest.

REFERENCES

Cai L, Gong Q, Qi L, Xu T, Suo Q, Li X, Wang W, Jing Y, Yang D, Xu Z, Yuan F, Tang Y, Yang G, Ding J, Chen H and Tian H (2022). ACT001 attenuates microglia-mediated neuroinflammation after traumatic brain injury via inhibiting AKT/NFκB/NLRP3 pathway. *Cell Commun Signal*., **20**(1): 56.

Cui X, Li X, He Y, Yu J, Dong N and Zhao RC (2021). Slight up-regulation of Kir2.1 channel promotes endothelial progenitor cells to transdifferentiate into a pericyte phenotype by Akt/mTOR/Snail pathway. *J Cell Mol. Med*., **25**(21): 10088–10100.

Feng L, Que D, Li Z, Zhong X, Yan J, Wei J, Zhang X, Yang P, Ou C and Chen M (2021). Dihydromyricetin ameliorates vascular calcification in chronic kidney disease by targeting AKT signaling. *Clin Sci (Lond)*., **135**(21): 2483–2502.

Feng Q, Yu X, Xie J, Liu F, Zhang X, Li S, Wang Y, Pan S, Liu D and Liu Z (2025). Phillygenin improves diabetic nephropathy by inhibiting inflammation and apoptosis via regulating TLR4/MyD88/NF-κB and PI3K/AKT/GSK3β signaling pathways. *Phytomedicine*., **136**: 156314.

Guan Y, Luan Y, Zhao S, Li M, Girolamo F, Palmer JD and Guan Q (2025). Single-cell RNA sequencing for characterizing the immune communication and iron metabolism roles in CD31+ glioma cells. *Transl. Cancer Res*., **14**(4): 2421–2439.

Guo M, He F and Zhang C (2024). Molecular therapeutics for diabetic kidney disease: An update. *Int J Mol Sci*., **25**(18): 10051.

Gupta S, Dominguez M and Golestaneh L (2023). Diabetic kidney disease: An update. *Med Clin North Am*., **107**(4): 689–705.

He D and Xu Y (2022). Toxicological evaluation of *Camellia euphlebia* leaves aqueous extract using acute and subacute toxicity studies in mice and genotoxicity studies. *Evid Based Complement Alternat Med*., **2022**: 7889199.

Hu X, Chen W, Yang M, Li M, Li X and Ouyang S (2025). IGFBP5 promotes EndoMT and renal fibrosis through H3K18 lactylation in diabetic nephropathy. *Cell Mol Life Sci*., **82**(1): 215.

Huang JC, Chen SC, Chang WA, Hung WW, Wu PH, Wu LY, Chang JM, Hsu YL and Tsai YC (2022). KITLG promotes glomerular endothelial cell injury in diabetic nephropathy by an autocrine effect. *Int J Mol Sci*., **23**(19): 11723.

Jacobs ME, de Vries DK, Engelse MA, Dumas SJ and Rabelink TJ (2024). Endothelial to mesenchymal transition in kidney fibrosis. *Nephrol Dial Transplant*,

39(5): 752–760.

Jing S, Qian J, Ying H, Mao P, Yao M, Wu Z, Bogaard HJ, Wang L, Li M and Yang J (2025). Activin a-activated ALK4 induces pathogenic Th17-involved endothelial-mesenchymal transition in systemic lupus erythematosus-associated pulmonary arterial hypertension. *Arthritis Rheumatol*., **77**(11): 1533–1547.

Karetnikova ES, Jarzebska N, Rodionov RN, Rubets E, Markov AG and Spieth PM (2023). mRNA levels of epithelial and mesenchymal markers in lung epithelial cell lines. *Rep Biochem Mol Biol*., **12**(2): 211–219.

Kushwaha K, Garg SS and Gupta J (2022). Targeting epigenetic regulators for treating diabetic nephropathy. *Biochimie*., **202**: 146–158.

Lee DJ, Lee JA, Chae DH, Jang HS, Choi YJ and Kim D (2022). Multiplex TaqMan qPCR assay for detection, identification and quantification of three sclerotinia species. *Mycobiology*, **50**(5): 382–388.

Li XZ, Jiang H, Xu L, Liu YQ, Tang JW, Shi JS, Yu XJ, Wang X, Du L, Lu Q, Li CL, Liu YW and Yin XX (2021). Sarsasapogenin restores podocyte autophagy in diabetic nephropathy by targeting GSK3β signaling pathway. *Biochem Pharmacol*., **192**: 114675.

Ouyang X, He, Z, Fang H, Zhang H, Yin Q, Hu L, Gao F, Yin H, Hao T, Hou Y, Wu Q, Deng J, Xu J, Wang Y and Chen C (2023). A protein encoded by circular ZNF609 RNA induces acute kidney injury by activating the AKT/mTOR-autophagy pathway. *Mol Ther*., **31**(6): 1722–1738.

Park JH and Choi YJ (2024). Designing A Novel Primer Set for GAPDH gene to enhance taxonomic and phylogenetic studies of Golovinomyces species. *Mycobiology*, **52**(4): 231–235.

Samsu N (2021). Diabetic nephropathy: Challenges in pathogenesis, diagnosis and treatment. *Biomed Res Int*., **2021:** 1497449.

Song S, Shi C, Bian Y, Yang Z, Mu L, Wu H, Duan H and Shi Y (2022). Sestrin2 remedies podocyte injury via orchestrating TSP-1/TGF-β1/Smad3 axis in diabetic kidney disease. *Cell Death Dis*., **13**(7): 663.

Su Q, Chen X, Ling X, Li D, Ren X, Zhao Y, Yang Y, Liu Y, He A, Zhu X, Yang, X, Lu W, Wu H and Qi Y (2023). SUMOylation of Smad2 mediates TGF-β-regulated endothelial-mesenchymal transition. *J Biol Chem*., **299**(10): 105244.

Sugahara M, Pak WL W, Tanaka T, Tang SCW and Nangaku M (2021). Update on diagnosis, pathophysiology and management of diabetic kidney disease. *Nephrology (Carlton)*., **26**(6): 491–500.

Tsuruta H, Yasuda-Yamahara M, Yoshibayashi M, Kuwagata S, Yamahara K, Tanaka-Sasaki Y, Chin-Kanasaki M, Matsumoto S, Ema M and Kume S (2024). Fructose overconsumption accelerates renal dysfunction with aberrant glomerular endothelial-mesangial cell interactions in db/db mice. *Biochim Biophys Acta Mol Basis Dis*., **1870**(4): 167074.

Xu Y, Ma X, Ni W, Zheng L, Lin Z, Lai Y, Yang N, Dai Z, Yao T, Chen Z, Shen L, Wang H, Wang L, Wu Y and Gao W (2024). PKM2-driven lactate overproduction triggers endothelial-To-mesenchymal transition in ischemic flap via mediating TWIST1 lactylation. *Adv Sci (Weinh)*., **11**(47): e2406184.

Xu Z, Jia K, Wang H, Gao F, Zhao S, Li F and Hao J (2021). METTL14-regulated PI3K/Akt signaling pathway via PTEN affects HDAC5-mediated epithelial-mesenchymal transition of renal tubular cells in diabetic kidney disease. *Cell Death Dis*., **12**(1): 32.

Yao L, Liang X, Liu Y, Li B, Hong M, Wang X, Chen B, Liu Z and Wang P (2023). Non-steroidal mineralocorticoid receptor antagonist finerenone ameliorates mitochondrial dysfunction via PI3K/Akt/eNOS signaling pathway in diabetic tubulopathy. *Redox Biol*., **68**: 102946.

Yin Z and Wang L (2023). Endothelial-to-mesenchymal transition in tumour progression and its potential roles in tumour therapy. *Ann Med*., **55**(1): 1058–1069.

Yoon JJ, Park JH, Lee YJ, Kim HY, Han BH, Jin HG, Kang DG and Lee HS (2021). Protective effects of ethanolic extract from rhizome of *Polygoni avicularis* against renal fibrosis and inflammation in a diabetic nephropathy model. *Int J Mol Sci*., **22**(13): 7230.

Zhang Y, Jin D, Kang X, Zhou R, Sun Y, Lian F and Tong X (2021). Signaling pathways involved in diabetic renal fibrosis. *Front Cell Dev Biol*., **9**: 696542.